minerals

MDPI

Article

The Paleozoic-Aged University Foidolite-Gabbro Pluton of the Northeastern Part of the Kuznetsk Alatau Ridge, Siberia: Geochemical Characterization, Geochronology, Petrography and Geophysical Indication of Potential High-Grade Nepheline Ore

Agababa A. Mustafaev [1,*], Igor F. Gertner [1], Richard E. Ernst [1,2], Pavel A. Serov [3] and Yurii V. Kolmakov [1,4]

1 Department of Geology and Geography, Tomsk State University, 634050 Tomsk, Russia; labspm@ggf.tsu.ru (I.F.G.); richard.ernst@ernstgeosciences.com (R.E.E.); kolmakovyv@tpu.ru (Y.V.K.)
2 Department of Earth Sciences, Carleton University, Ottawa, ON K1S 5B6, Canada
3 Laboratory of Geochronology and Isotope Geochemistry, Kola Scientific Center of the Russian Academy of Sciences, 184209 Apatity, Russia; serov@geoksc.apatity.ru
4 Department of Geology and Geophysics, Tomsk Polytechnic University, 634050 Tomsk, Russia
* Correspondence: alishka010593@gmail.com; Tel.: +7(913)-866-88-24

Received: 30 October 2020; Accepted: 13 December 2020; Published: 15 December 2020

Abstract: Geological, geochemical and ground magnetic techniques are used to characterize the University alkaline-gabbroid pluton and crosscutting N-S trending alkaline dikes, located northeast of the Kuznetsk Alatau ridge, Siberia. Trace element concentrations and isotopic compositions of the igneous units were determined by XRF, ICP-MS and isotope analysis. The Sm-Nd age of subalkaline (melanogabbro, leucogabbro 494–491 Ma) intrusive phases and crosscutting alkaline dikes (plagioclase ijolite, analcime syenite 392–389 Ma) suggests two stages of activity, likely representing separate events. The subalkaline and alkaline rocks are characterized by low silicic acidity (SiO_2 = 41–49 wt %), wide variations in alkalinity ($Na_2O + K_2O$ = 3–19 wt %; Na_2O/K_2O = 1.2–7.2 wt %), high alumina content (Al_2O_3 = 15–28 wt %) and low titanium content (TiO_2 = 0.07–1.59 wt %). The new trace element data for subalkaline rocks (∑REE 69–280 ppm; La/Yb 3.7–10.2) of the University pluton and also the crosscutting younger (390 Ma) alkaline dikes (∑REE 10–1567 ppm; La/Yb 0.7–17.8 ppm) both reflect an intermediate position between oceanic island basalts (OIBs) and island arc basalts (IABs). The presence of a negative Nb–Ta anomaly and the relative enrichment in Rb, Ba, Sr, and U indicate a probable interaction of mantle plume material with the lithospheric mantle beneath previously formed accretion complexes of subduction zones. The isotopic signatures of strontium (ε_{Sr}(T) +3.13–+28.31) and neodymium (ε_{Nd}(T) +3.2–+8.7) demonstrate the evolution of parental magmas from a plume source from moderately depleted PREMA mantle, whose derivatives underwent selective crustal contamination.

Keywords: magnetometry; alkaline-gabbroid association; Rb-Sr and Sm-Nd geochronology; plume lithospheric interaction; Kuznetsk Alatau; Central Asian Orogenic Belt

1. Introduction

Alkaline magmatism has been long considered to be typical of platformal settings, and where it occurred within folded regions, and then it was given secondary importance. Various origins have been considered: (1) under conditions of a quiet tectonic regime (platform, postorogenic), differentiation of mafic magmas resulting in the formation of small volumes of residual alkaline melts [1–3]; (2) an

association with extensional processes and more specifically with rifting events [4,5] and (3) a link with plume activity [6,7]. We consider the setting of alkaline magmatism in the Central Asian Orogenic Belt (CAOB) [8–35] developing from the Neoproterozoic to the Late Paleozoic [36–42].

In the western CAOB, the large Altai-Sayan orogenic system [43] frames the southern part of the Siberian craton. This system includes several smaller terranes, such as the Kuznetsk Alatau (KA), Western and Eastern Sayan, Tuva-Sangilen and Tuva-Mongolian [44,45]. The KA is a Caledonian terrane dominated by accretionary structural-material complexes belonging to the active margin of the Paleo-Asian Ocean [22], where Paleozoic alkaline basic magmatism (volcanic, subvolcanic and intrusive) is extensive [45,46] and at least two pulses of regional intraplate magmatic activity are present: ca. 500 Ma picrite and picrodolerite magmatism, and younger widespread magmatism [47] and associated rifts dated ca. 400 Ma, which have been called the Altai-Sayan Rift System and the Altai-Sayan LIP (Large Igneous Province) [43,48]. This magmatism includes small (up to 1–3 km^2) differentiated alkaline-basic plutons, composed of different proportions of subalkaline and alkaline gabbro, basic and ultrabasic foidolites, nepheline and alkaline syenites (Figure 1b).

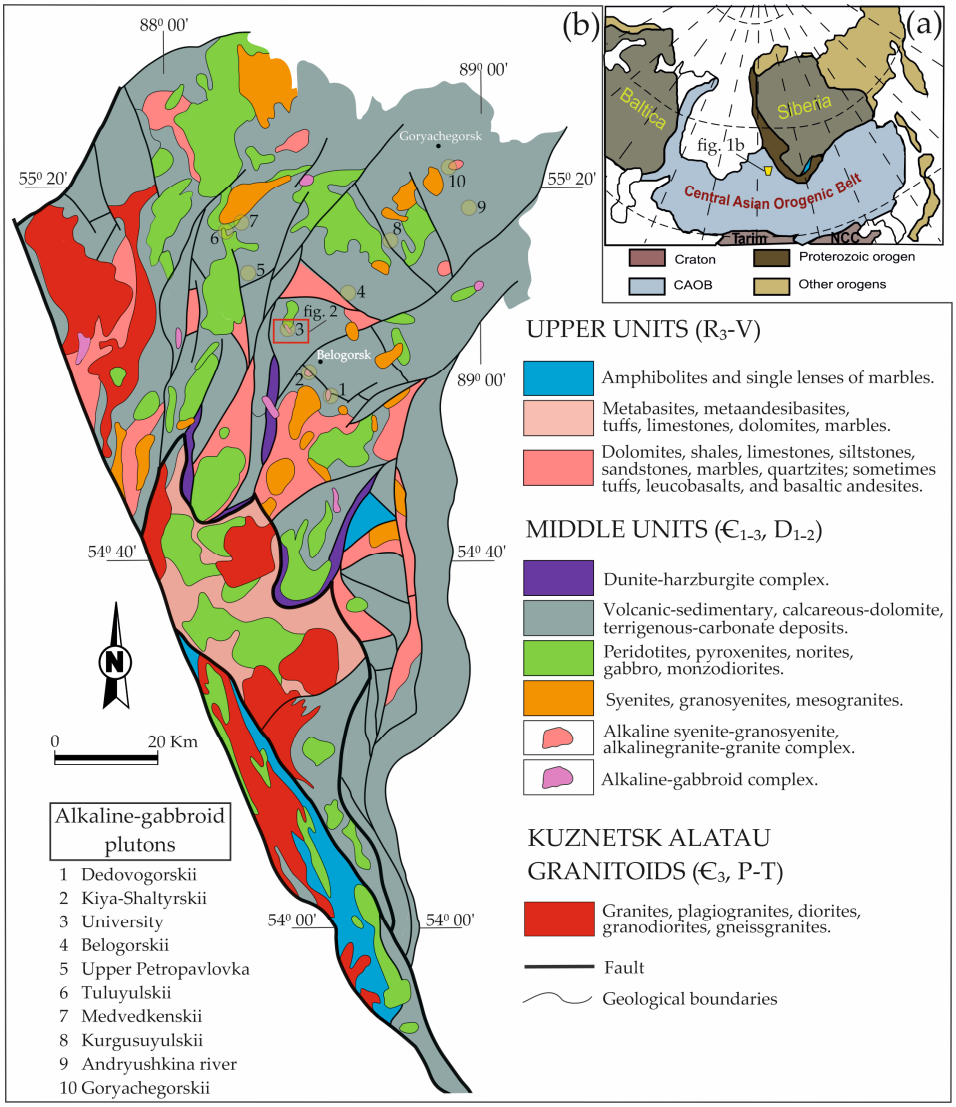

Figure 1. Simplified scheme of the Central Asian orogenic belt (**a**) after [34,49,50] with a fragment of the geological map of the northern part of the Kuznetsk Alatau (KA) ridge and (**b**) after [51] with changes and additions by the authors. Red box locates Figure 2 and Figure 4.

This paper will highlight our results on the University pluton, which contributes to an understanding of the regional alkaline magmatism in this CAOB terrane. The University pluton and surrounding region are discussed in detail including their magnetic expression, and the petrology and geochemistry of the various magmatic units, which include subalkaline gabbroids, leucotheralites and basic and ultrabasic foidolites, to determine the time and conditions of formation of the University pluton and crosscutting alkaline dikes.

2. Geology and Petrography of the University Pluton

The Kuznetsk Alatau (KA) terrane is a typical Early Caledonian (Salairian) tectonic terrane, with folding processes completing in the middle-upper Cambrian [52,53]. This area also includes inliers of Precambrian basement, a system of troughs and uplifts of the Salair orogen and superimposed Middle Paleozoic rift basins belonging to the Altai-Sayan Rift/LIP system [43,48].

The University pluton (N55°05′30″, E88°23′30″) is an inlier localized in a small erosion window (0.86 km^2) of Early Cambrian carbonate deposits, which are overlapped by Middle Cambrian volcanic rocks. The pluton is poorly exposed and partially overlain by large-blocks of deluvium deposits derived from erosion of the Voskresenskii gabbro-diorite-granodiorite intrusion (presumably Upper Cambrian) from the northern part of the area. The contacts of the pluton are almost everywhere tectonic with gabbroids and plagiogranites of the Voskresenskii intrusion. The pluton shape resembles a stock (2.5 × 0.2–0.6 km, with a total area of 0.53 km^2), significantly complicated by faults (Figure 2). The Ust-Kundat Formation of the Lower Cambrian is composed of limestones with interlayers of clay shales, sandstones, tuffs and metavolcanics of andesite-basaltic composition. Volcanic units consisting of basalts of andesite-basalts, dacites and tuffs of the Middle Cambrian Berikul Formation are widespread in the region, and occur with an angular unconformity with underlying rocks.

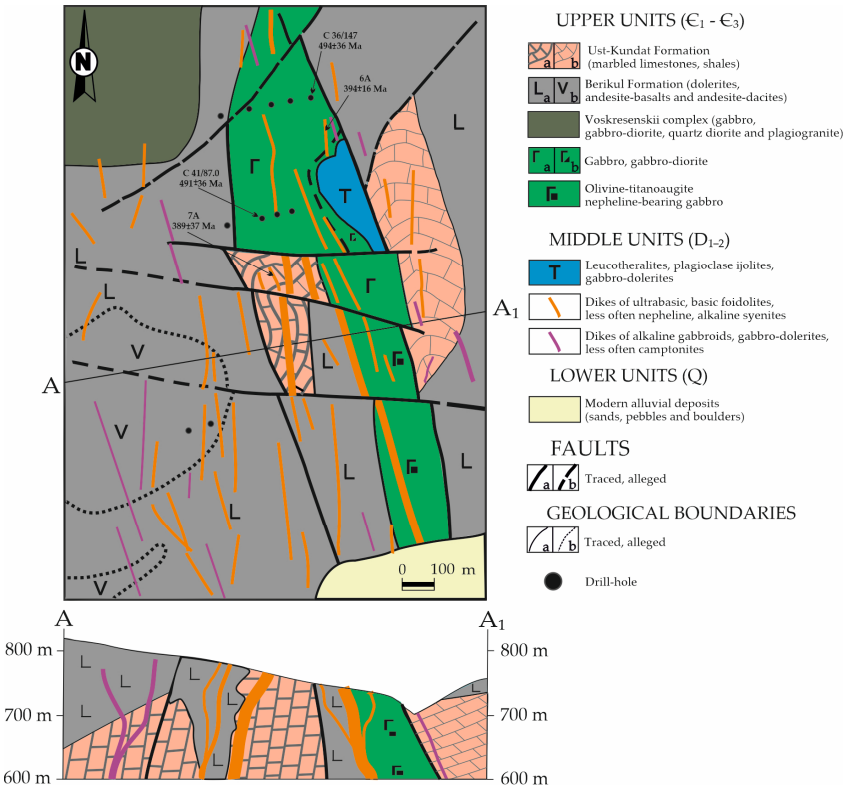

Figure 2. Simplified scheme of the geological structure and a section along the A-A$_1$ line of the University pluton on a scale of 1:5000 according to [54,55] with the additions by the authors. The center of the image is at about N55°05′30″, E88°23′30″.

The petrographic varieties of the pluton are represented mainly by subalkaline gabbroids (Figure 3a,b) and their subvolcanic analogs (subalkaline gabbro-dolerites). In the northeastern part of the University pluton, subalkaline gabbroids cut bodies of feldspar ijolites containing local zones of leucotheralites (Figure 3c,d). The crosscutting N-S-trending dikes are represented by a wide variety of compositions: ultrabasic foidolites (urtite-porphyry, microijolites with inclusions of urtites and ijolite-porphyry; Figure 3e,f), basic foidolites (plagioclase ijolite and plagioclase ijolites with varying degrees of crystallization with globules of analcime syenites; Figure 3g), nepheline microsyenites containing varieties of the tamaraites type) and subalkaline plagioclase porphyrites [32,54,55].

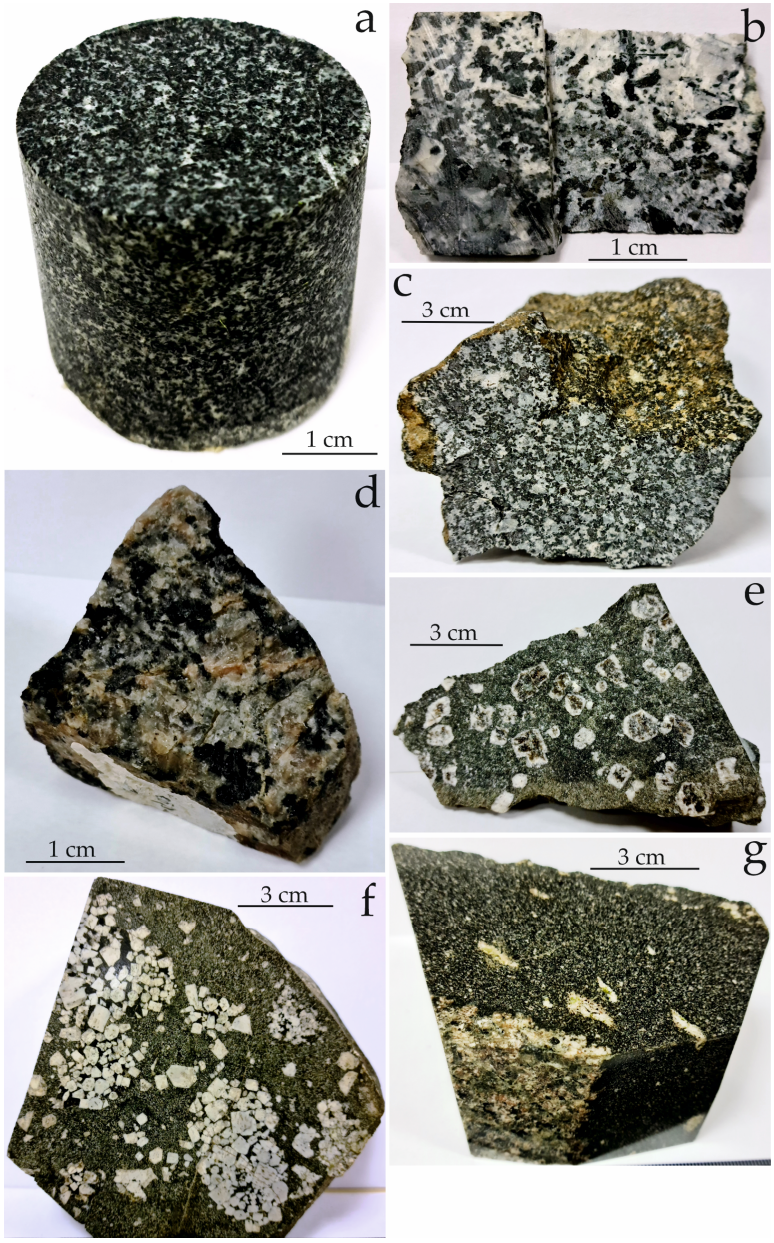

Figure 3. Macrophotography of the main petrographic varieties of the University pluton: (**a**) melanogabbro (sample 36/147.0) and (**b**) leucogabbro (sample 41/87.0); and the crosscutting N-trending dike rocks: (**c**) plagioclase ijolite (sample 6A); (**d**) leucotheralite (sample 8A); (**e**) ijolite-porphyry (sample 8/19); (**f**) urtite xenolith in ijolite-porphyry (sample KC-7/1) and (**g**) analcime syenite (globule) in fine-grained ijolite (sample 7A).

3. Materials and Methods

Ground magnetic prospecting at the University pluton site was carried out in 1983 with an M-27 optical-mechanical magnetometer with the measurement of the vertical component of the magnetic field vector in gammas [56]—units of the CGS system: 1 gamma = 10^{-5} oersted (Oe). In modern research, magnetic field maps are plotted according to the values of magnetic induction, measured in nT. 1 nT = 10^{-9} T are SI units of magnetic induction. 1 Oe is numerically equal to 10^{-4} T. In this article, the magnetic survey results are presented in modern concepts based on the calculation that 1 gamma is numerically equal to 1 nT.

The concentrations of petrogenic and rare trace elements were measured by XRF at the Institute of Geology and Mineralogy V.S. Sobolev Siberian Branch of the Russian Academy of Sciences (Novosibirsk, Russia) on spectrometer ARL-9900XP and by ICP-MS at Tomsk State University (Tomsk, Russia) on spectrometer Agilent 7500.

X-ray fluorescence silicate analysis was performed from fused pellets: the analyzed sample was dried at 105 °C for 1.5 h, then annealed at 960 °C for 2.5 h and then mixed with flux (66.67% lithium tetra borate; 32.83% lithium meta borate and 0.5% lithium bromide) in a ratio of 1:9 (the total weight of the mixture was 5 g). The mixture was melted in platinum crucibles in a Lifumat-2.0-Ox induction furnace according to the standard method [57].

To perform mass spectral analysis with inductively coupled plasma, a 0.1 g sample was treated with 10 mL of HF acid with 4-h exposure in an open system at a temperature of 70 °C, after which 2 mL of HNO_3 concentrate was added. The samples were exposed to microwave action in a closed system at a power of 700 W with a gradual increase in temperature to 200 °C. After this, the sample was evaporated to dryness, treated twice with 6.2 M HCl, then evaporated again and treated with concentrated HNO_3. Then the dry residue was transferred to a solution of 15% HNO_3. Indium was used as an internal standard. Immediately prior to ICP-MS measurements, the sample was diluted by nitric acid to yield a concentration 3%. The dilution factor was 1000 [58].

Sm-Nd and Rb-Sr-isotope analysis was carried out at the Geological Institute of the Kola Science Center of the Russian Academy of Sciences (Apatity, Russia) using Finnigan-MAT-262 (RPQ) and MI-1201-T mass spectrometers in a static measurement mode according to the adopted method [59]. Measurements of the JNdi-1 standard [60] yielded $^{143}Nd/^{144}Nd = 0.512081 \pm 13$ ($N = 11$) for gabbro and $^{143}Nd/^{144}Nd = 0.512090 \pm 13$ ($N = 9$) for alkaline rocks. The analytical error (2σ) does not exceed 0.5% for $^{147}Sm/^{144}Nd$, 0.005% for $^{143}Nd/^{144}Nd$ [61]. The Sr isotopic composition was normalized to the values of the NBS SRM-987 standard ($^{87}Sr/^{86}Sr = 0.710235$) [62]. The error in determining the Sr concentration is 0.04% and the Rb–Sr ratio was 1.5%. To calculate the primary isotopic ratios, ε_{Nd}, ε_{Sr}, the modern parameters of the model reservoirs CHUR ($^{143}Nd/^{144}Nd = 0.512630$, $^{147}Sm/^{144}Nd = 0.1960$) [63] and UR ($^{87}Sr/^{86}Sr = 0.7045$; $^{87}Rb/^{86}Sr = 0.0816$) [64] were used. The construction of isochrones was carried out by the method of D. York [65] using the Isoplot/Ex program [66].

4. Results

4.1. The Magnetic Field of the University Pluton Site

As noted above, the University pluton is poorly exposed, and in order to properly delineate it, both geological mapping (boreholes, pits and ditches) and a ground magnetic survey were used [56]. The magnetic map (based on the ground survey; Figure 4) revealed both the University pluton and crosscutting N-trending dike rocks by elevated values which range from +15 to +150 nT. The zone is characterized by a complex structure, but it stands out quite well against the background values of −10 to −50 nT, created by non-magnetic host sedimentary rocks of the Ust-Kundat and Berikul formations.

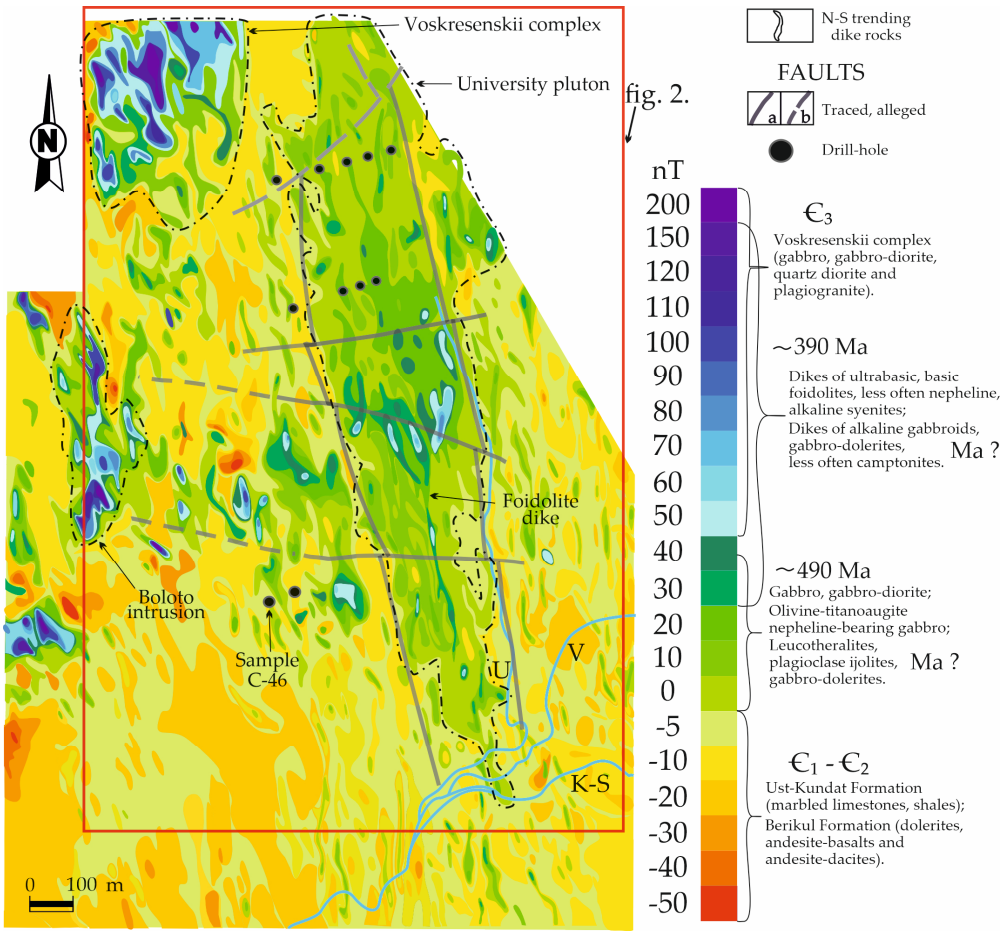

Figure 4. Magnetic map of the University pluton at a scale of 1:5000 based on ground survey by [56] with processing by the authors. K-S = Kiiskii-Shaltyr river; V = Voskresenka stream; U = University stream. Same area as in Figure 2. The center of the image is at about N55°05′30″, E88°23′30″. Red box locates Figure 2.

Values of the magnetic field up to +30 nT are observed over subalkaline gabbroids and gabbro-dolerites that are part of the University pluton. The N-trending dikes of ultrabasic and basic foidolites occur as linear anomalies with amplitudes of +30–+80 nT, and in some cases up to +80–+150 nT. A high-intensity +50–+200 nT anomaly located northwest of the University pluton is associated with gabbro-diorites and plagiogranites of the Voskresenskii intrusion (Figure 4). The submeridional linear anomaly with amplitude of more than +200 nT on the western flank of the University pluton is of interest as deposits of nepheline ores, and we gave it the name, Boloto intrusion (Figure 4). In its shape, it is similar to the anomalies from the N-S dikes cutting the University pluton, but typically with almost twice the amplitude.

4.2. Main Petrographic Varieties of the University Intrusion Site

The petrographic description is provided only for the main units of the University pluton for which geochemical and isotope-geochronological studies were carried out.

Subalkaline melanocratic gabbro (N55°05′48″, E88°23′47″) is widespread in the eastern and northeastern parts of the pluton (Figure 2). It is a gray to dark gray rock with a medium grain structure and taxite texture (Figures 3a and 5a). The thin section contains hypidiomorphic-grained, poikilitic and poikilophyte structures, of which titanoaugite grains (Fs_{14}) had a higher degree of idiomorphic than plagioclase (An_{37-67}). This unit has a noticeably higher content of dark-colored mineral components by

10–15%. Olivine (Fo_{58-67}) is present in significant amounts up to 10% and has large idiomorphic grains. Minor minerals are titanomagnetite, apatite, hornblende and serpentine.

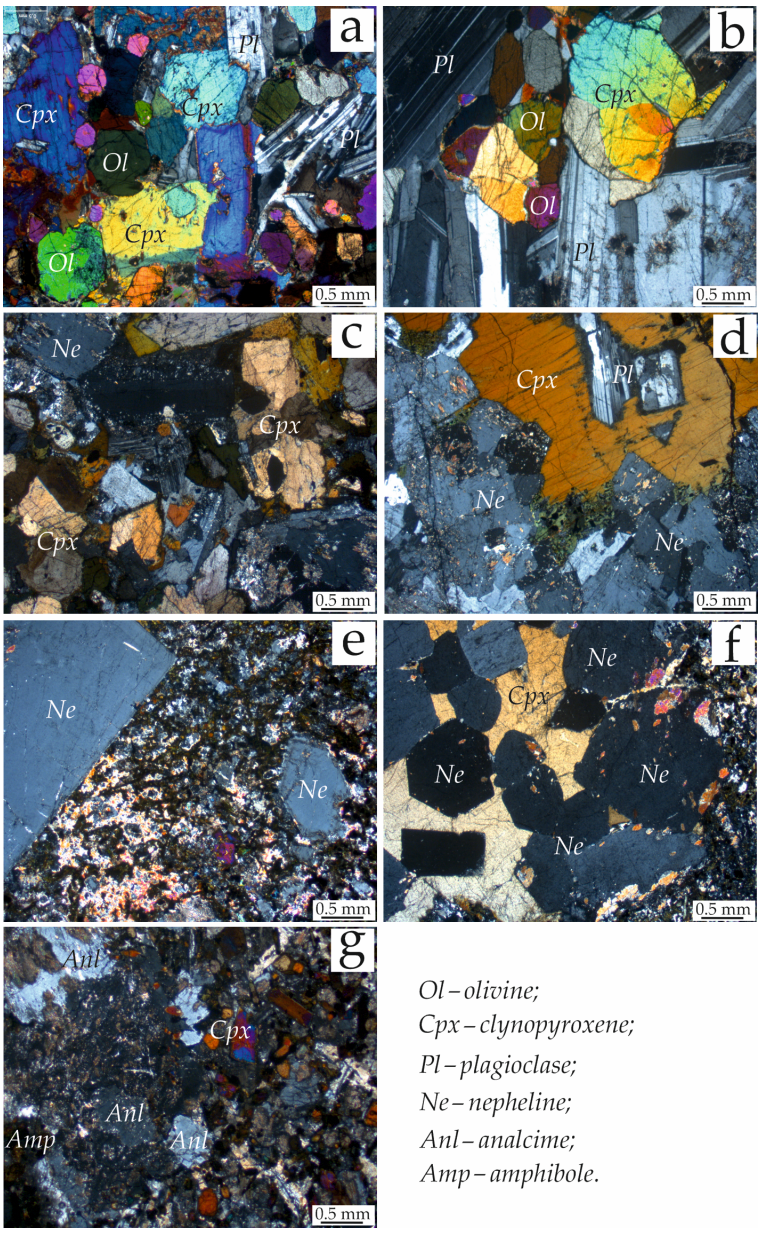

Figure 5. Photomicrographs of samples from the University pluton and crosscutting N-trending dikes: (**a**,**b**) subalkaline melanogabbro (sample C36/147.0) and leucogabbro (sample C41/87.0) mainly consist of clinopyroxene, plagioclase and olivine in different proportions and are characterized by a hypidiomorphic to ophitic structure; and the crosscutting N-trending dikes: (**c**) plagioclase ijolite (sample 6A) consists of nepheline, clinopyroxene, plagioclase and titanomagnetite with a distinct hypidiomorphic granular texture; (**d**) leucotheralite (sample 8A) consists of nepheline, clinopyroxene and plagioclase and is represented by a hypidiomorphic granular texture and (**e**,**f**) ijolite-porphyry (sample 8/19) and urtite xenolith in ijolite-porphyry (sample KC-7/1) are composed of nepheline and clinopyroxene in different proportions and are represented by a porphyry texture. The matrix of ijolite porphyry in which the urtite xenolith is placed is represented by a microhypidiomorphic-grained texture; (**g**) analcime syenite (globule) in fine-grained ijolite (sample 7A) consists of analcime, alkaline feldspar and amphibole with a hypidiomorphic-grained texture.

Subalkaline leucocratic gabbro (N55°05′34″, E88°23′39″) is the most widespread unit and forms the central and western parts of the pluton (Figure 2). In appearance, these gabbroids are gray and light gray, medium and coarse-grained leucocratic rocks, and often exhibit a trachytic texture defined by the sub parallel arrangement of elongated plagioclase crystals (Figures 3b and 5b). Ophitic, less often poikilitic textures, with a pronounced idiomorphic shape of the main plagioclase (An_{48-62}) more than the pyroxene is characteristic. Pyroxene has a light gray and yellow-greenish color (Fs_{10-11}). Olivine is found in this section less than in the melanocratic variety and is represented by hyalosiderite (Fo_{34-47}). Accessory minerals include titanomagnetite, sometimes apatite and calcite.

Plagioclase ijolites or theralites, leucotheralites (basic foidolites; N55°05′40″, E88°24′54″) corresponding to the second magmatic series, compose rather large the N-S dikes up to 40 m thick and a separate intrusive body in the northeast of the pluton with an area of up to 0.4 km^2 (Figure 2). In appearance, plagioclase ijolite is represented by fine- and medium-grained, massive or weakly taxite rock of melanocratic (dark gray) appearance (Figures 3c and 5c). A hypidiomorphic granular structure is observed under the microscope. Mineralogical composition: nepheline 40% (Ks_{22}), ferrosilite 35% (Fs_{23}), plagioclase 15% (An_{41-63}) and titanomagnetite up to 8%. Hornblende, apatite, analcime and calcite are minor minerals 2%. Leucotheralite is a light gray coarse-grained leucocratic rock with hypidiomorphic-grained and poikilitic micro texture (Figures 3d and 5d). The unit consists of nepheline 42% (Ks_{20-25}), salite 37% and plagioclase 19% (An_{50-55}). Hornblende (large single grains), biotite, titanomagnetite and apatite are present as minor minerals 2%.

Ijolite-porphyries and micro-ijolites (N55°05′37″, E88°24′00″) are feldspar-free fine-grained dark gray rocks, sometimes with a greenish tint. On visual observation, they are well defined by regular nepheline large crystals 2–40 mm (Figures 3e and 5e) defining a porphyritic texture. Nepheline 50–55% (Ks_{20}) is transparent and has a greenish and brownish color, however, it is more often replaced by libenerite, spreushtein and limonite. Pyroxene is represented by aegirine-augite, less often by titanoaugite 35–40% (Fs_{23}). Minor minerals in the amount of up to 5% include titanomagnetite and apatite.

Ijolite-porphyries with urtite xenoliths (N55°04′54″, E88°23′00″) are distinguished by the presence of schlieren segregates of fully-crystalline urtites from fine to coarse-grained and pegmatoid in texture (Figures 3f and 5f), rounded and slightly elongated in shape up to 5–8 cm in size, which we consider as urtite xenoliths. Under the microscope, the agpaitic structure of ijolite-urtite is clearly visible, which is composed of 65–80% nepheline (Ks_{20-25}), ferrosilite 18–33% (Fs_{22-26}) with a slight admixture of 2% titanomagnetite and apatite.

The analcime syenite (globule) in the plagioclase fine-grained ijolite (N55°04′41″, E88°24′00″) has a light gray to dark green color, fine-grained (bulk) and medium-grained (globule) structures, and massive texture (Figures 3g and 5g). In the thin section, the globule is represented by a trachytic texture with a mineral composition: analcime 27%, alkaline feldspar 35%, amphibole 35% and minor minerals 3% apatite and sphene.

In the central-western area of the University pluton, the drill hole material from approximately 100 m depth shows the presence of urtite-porphyry dikes N-trending (up to 7 cm in size) in the core (N55°04′60″, E88°23′06″; the location of the sample C-46 can be seen in Figure 4; Figure 6a). These are independent dikes that cut the ijolite-porphyries, and volcanic strata of the Berikul Formation and provide proof of the existence of a direct genetic relationship between ijolites and urtites, and the formation of urtites as a result of crystallization differentiation from an ijolite melt [45].

The intrusive nature of the relationship of gabbroids with host volcanic rocks can be observed from the same deluvium clastic material, in which acute-angled xenoliths of basaltic clastic rock are clearly recorded as xenoliths in gabbroids (N55°05′17″, E88°24′24″) of the pluton (Figure 6b).

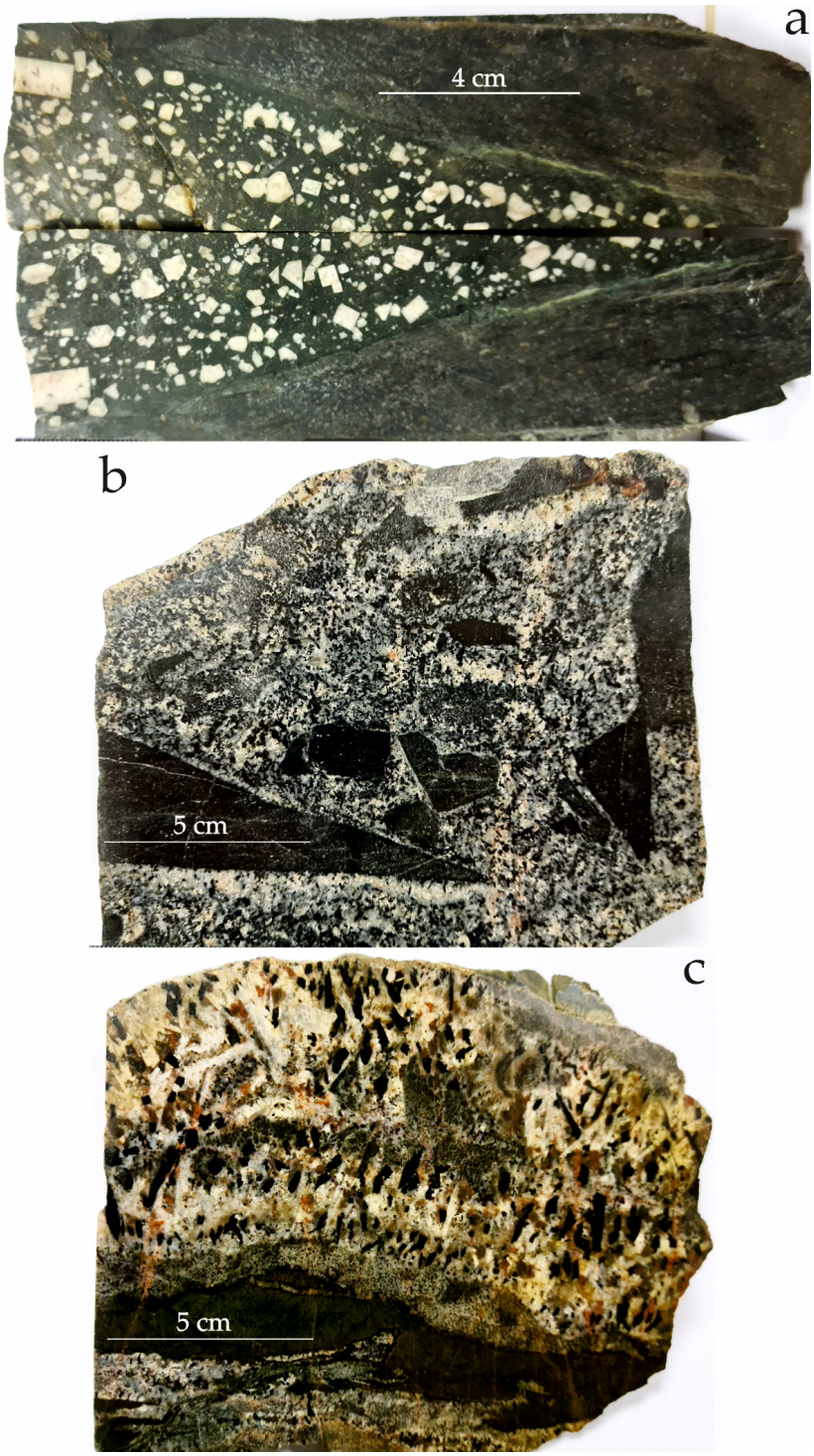

Figure 6. Hand sample photographs of some small dikes N-trending belonging to the University pluton: (**a**) an urtite-porphyry dike intersecting the volcanogenic deposits of the Berikul Formation in the core of the drill hole (sample C-46); (**b**) subalkaline gabbro with xenoliths of brecciated basalt fragments (sample UN-2/1) and (**c**) veinlet's of pegmatoid nepheline syenite in feldspar micro-ijolite, which cut the ijolite plagioclase (sample 15B).

In some dikes, nepheline syenites (N55°04′45″, E88°23′14″) and microsyenites are noted, which cut thin veins of ijolite plagioclase (Figure 6c).

4.3. Major- and Trace-Element Compositions of Subalkaline and Alkaline rocks

The igneous rocks of the University pluton are characterized by low silicic acidity (SiO_2 = 41–49 wt %), wide variation in alkalinity ($Na_2O + K_2O$ = 3–19 wt %; Na_2O/K_2O = 1.2–7.2 wt %), low titanium content (TiO_2 = 0.07–1.59 wt %) and high alumina content (Al_2O_3 = 15–28 wt %), which corresponds to K-Na derivatives of the basic alkaline formation (Figure 7a; Table S1). The average compositions of the main varieties are plotted on the APF diagram (Figure 7b). The rocks of the pluton were divided into four groups according to their mineralogical composition: subalkaline gabbroids (ca. 490 Ma), foidolites, syenites (N-S dikes of ca. 390 Ma) and leucotheralites (there was no data on age, but we linked their formation with N-S dikes of ca. 390 Ma), which occupy an intermediate position in composition between gabbroids and foidolites.

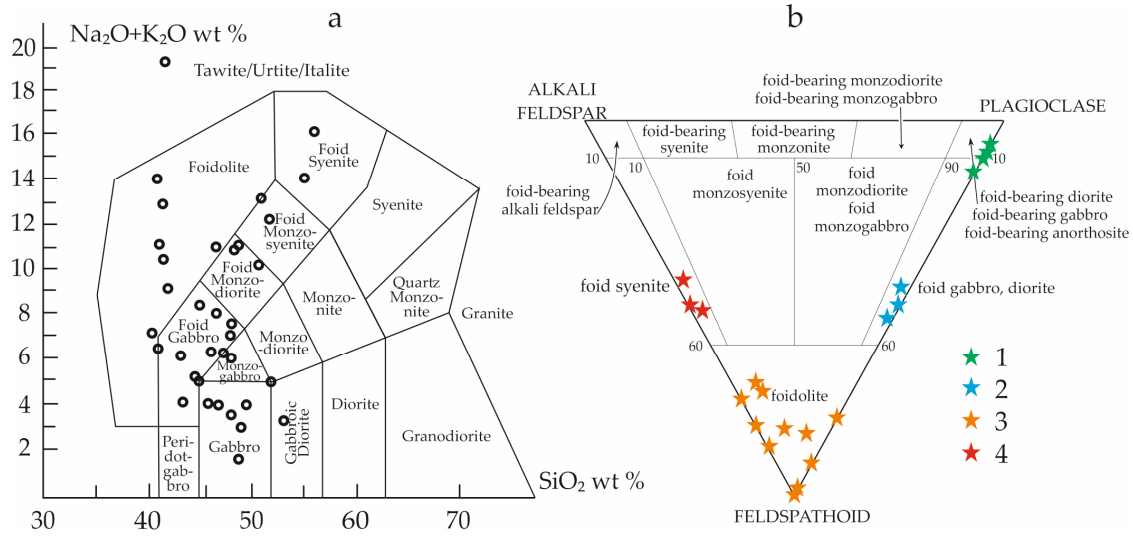

Figure 7. Classification of silicate rocks of the University pluton. (**a**) On the (TAS) diagram, the classification fields are given according to [67] and (**b**) classification of plutonic rocks in the system (APF) according to modal content of minerals in volume percent according to [68]. The stars indicate: 1 = subalkaline gabbro ca. 490 Ma and subalkaline gabbro-dolerites; 2 = leucotheralites; 3 = foidolites ca. 390 Ma; 4 = nepheline and alkaline syenites ca. 390 Ma.

The units of the University pluton are characterized by lanthanide values of La/Yb(n) and by the sum of rare earth elements ∑REE (subalkaline gabbroids La/Yb(n) = 2.68–6.97, ∑REE = 64.09–236.65 ppm; leucotheralites La/Yb(n) = 4.90–7.37, ∑REE = 135.48–279.83 ppm; foidolites La/Yb(n) = 0.53–12.74, ∑REE = 10.02–217.61 ppm; nepheline and alkaline syenites La/Yb(n) = 5.14–9.07, ∑REE = 73.24–1566.96 ppm; Table S1). The enrichment of light rare earth elements (LREE) relative to heavy rare earth elements (HREE) was characteristic of all samples (Figure 8).

4.4. Nd–Sr Isotope Systematics

Subalkaline, alkaline rocks of the University pluton had common values of primary isotopes of neodymium $^{143}Nd/^{144}Nd(t)$ = 0.512223–0.512358 and $\varepsilon_{Nd}(T)$ ranging from +3.2 to +8.7 and, possibly, originated from the moderately depleted mantle type (PREMA) with crustal enrichment of the primary strontium isotope ratio $^{87}Sr/^{86}Sr(t)$ = 0.704834–0.706037 and $\varepsilon_{Sr}(T)$ from +12.93 to 28.31 (Figure 9, Table 1). Enrichment in radiogenic ^{87}Sr was found for many Paleozoic-Mesozoic alkaline and carbonatite complexes in the northern part of the Kuznetsk Alatau, Southeastern Tuva, and the southeastern part of the Russian Altai [31].

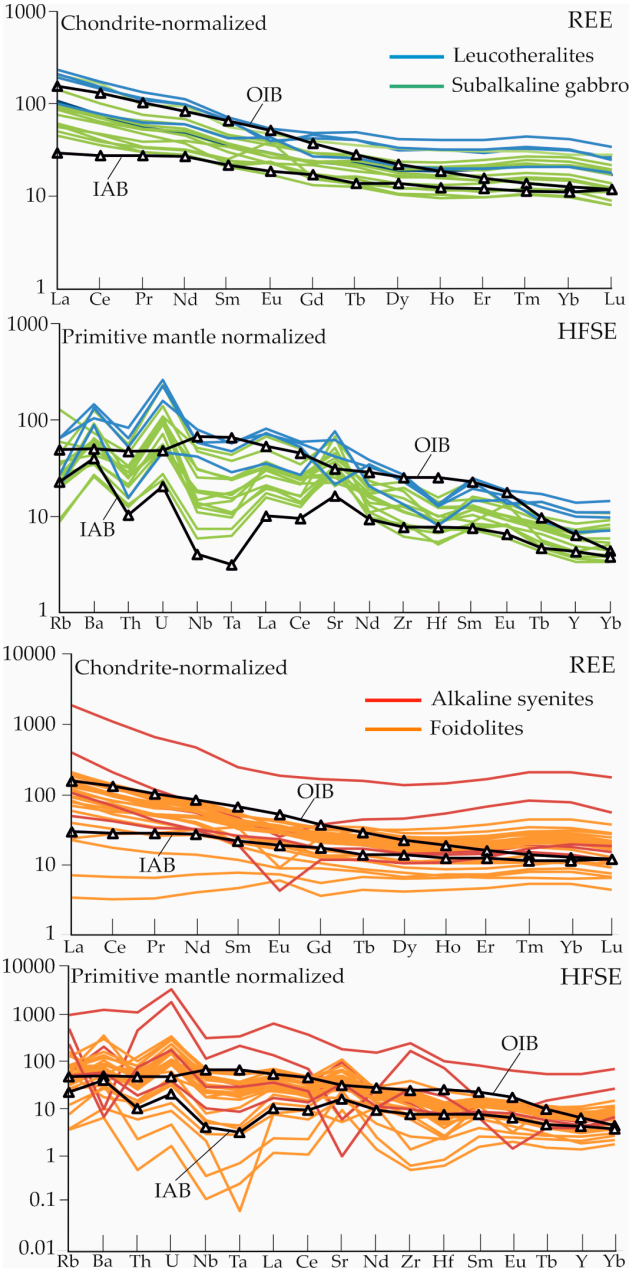

Figure 8. Chondrite-normalized rare earth elements (REE) and primitive mantle normalized high-field-strength elements (HFSE) [69] igneous rocks of the University pluton. The oceanic island basalt (OIB) spectrum line is given in [69], island arc basalt (IAB) in [70]. Subalkaline gabbro ca. 490 Ma; leucotheralites (there is no data on age, but we link their formation with N-S dikes of ca. 390 Ma); alkaline syenites and foidolites ca. 390 Ma.

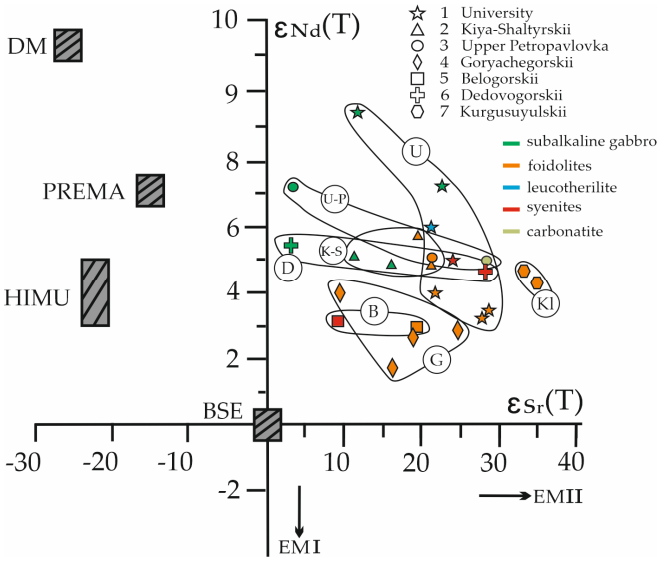

Figure 9. A plot of εNd(T) versus εSr(T) for the University pluton and some other alkaline-basic complexes of the northern part of the KA ridge: 1 = University (U); 2 = Kiya-Shaltyrskii (K-S) after [21]; 3 = Upper Petropavlovka (U-P) after [9]; 4 = Goryachegorskii (G) after [31]; 5 = Belogorskii (B), after [8]; 6 = Dedovogorskii (D) and 7 = Kurgusuyulskii (Kl) after [21]. Positions of reservoirs DM (depleted mantle); PREMA (dominant mantle); HIMU (mantle with high U/Pb ratio); BSE (bulk composition of silicate Earth) and EM I and EM II (two types of enriched mantle characterized by high values of $^{143}Nd/^{144}Nd$ and $^{87}Sr/^{86}Sr$) are given according to their current isotopic parameters [71].

Table 1. Nd-Sr isotopic composition of subalkaline unit's ca. 490 Ma of the University pluton and younger crosscutting N-S alkaline dike swarm ca. 390 Ma.

Sample, Rock	Sm, ppm	Nd, ppm	$^{147}Sm/^{144}Nd$	$^{143}Nd/^{144}Nd \pm 2\sigma$	$(^{143}Nd/^{144}Nd)_T$	$\varepsilon_{Nd}(T)$
C-41/87.0(WR), LG	1.769	7.462	0.143307	0.512907 ± 12	0.512355	+8.7
Pl	0.588	3.44	0.1033	0.512797 ± 9		
Ol	3.95	11.02	0.2165	0.513160 ± 12		
Px	2.43	7.99	0.1841	0.513041 ± 25		
C-36/147.0(WR), MG	3.418	15.266	0.135334	0.512808 ± 9	0.512358	+7.3
Pl	1.531	9.458	0.0978	0.512709 ± 16		
Ol	4.49	13.23	0.2050	0.513051 ± 10		
Px	4.18	15.02	0.1682	0.512922 ± 8		
AC-7/1(WR), AS	6.614	20.709	0.153049	0.512221 ± 9	0.512271	+4.0
УН-1(WR), U	3.981	22.298	0.107919	0.512693 ± 7	0.512273	+3.5
8a(WR), LT	2.906	16.428	0.106922	0.512667 ± 19	0.512223	+4.9
6a(WR), I	6.61	20.7	0.1530	0.512692 ± 12	0.512236	+3.2
Px	8.38	29.9	0.1693	0.512745 ± 5		
Ne	0.689	4.11	0.1015	0.512569 ± 25		
7a(WR), AS	3.98	22.3	0.1079	0.512694 ± 13	0.512291	+5.8
Pl	0.469	3.2	0.0887	0.512621 ± 12		
Amp	12.91	50.8	0.1536	0.512794 ± 11		
Anl	0.93	5.59	0.1006	0.512664 ± 8		
Sample, Rock	**Rb ppm**	**Sr ppm**	$^{87}Rb/^{86}Sr$	$^{87}Sr/^{86}Sr \pm 2\sigma$	$(^{87}Sr/^{86}Sr)_T$	$\varepsilon_{Sr}(T)$
C-41/87.0(WR), LG	13.75	744.94	0.052077	0.70520 ± 20	0.704834	+12.93
C-36/147.0(WR), MG	19.33	582.49	0.093628	0.70620 ± 23	0.705541	+22.99
AC-7/1(WR), AC	47.49	1261.1	0.106247	0.70615 ± 22	0.705556	+21.48
УН-1(WR), U	54.1	1414.8	0.107886	0.70664 ± 19	0.706037	+28.31
8a(WR), LT	44.3	963.86	0.129674	0.70649 ± 20	0.705766	+24.44
6a(WR), I	23.46	1023.7	0.064658	0.70633 ± 21	0.705969	+27.34
7a(WR), AS	36.42	2542.9	0.040409	0.70574 ± 16	0.705514	+20.87

Note. LG = subalkaline leucogabbro and MG = subalkaline melanogabbro ca. 490 Ma; KC = urtite xenolith in ijolite-porphyry, U = urtite-porphyry, LT = leucotheralite, I = plagioclase ijolite and AS = analcime syenite (globule) in fine-grained ijolite ca. 390 Ma. WR, whole-rock composition, Pl, plagioclase, Ol, olivine, Px, pyroxene, Ne, nepheline, Amp, amphibole, Anl, analcime. $(^{143}Nd/^{144}Nd)_T$ and $\varepsilon_{Nd}(T)$ are calculated for the age of 490 Ma for melanogabbro and leucogabbro and 392 Ma for plagioclase ijolite and analcime syenite.

The ages of the University pluton and associated N-S dike swarm were determined by Sm-Nd dating of minerals and whole compositions. The two samples from the main phase of the pluton yielded

ca. 490 Ma ages for the subalkaline gabbro (melanogabbro 494 ± 36 Ma; leucogabbro 491 ± 36 Ma). The second phase of crosscutting N-S trending alkaline dikes had ca. 390 Ma age's (plagioclase ijolite 394 ± 16 Ma; analcime syenite 389 ± 37 Ma; Figure 10). These approximate ages suggest that the University pluton belongs ca. 500 Ma event, which is widespread in Mongolia (Figure 6 in [20,47]), while the crosscutting N-S dikes belong to the ca. 400 Ma Altay-Sayan Rift/LIP event [43,48].

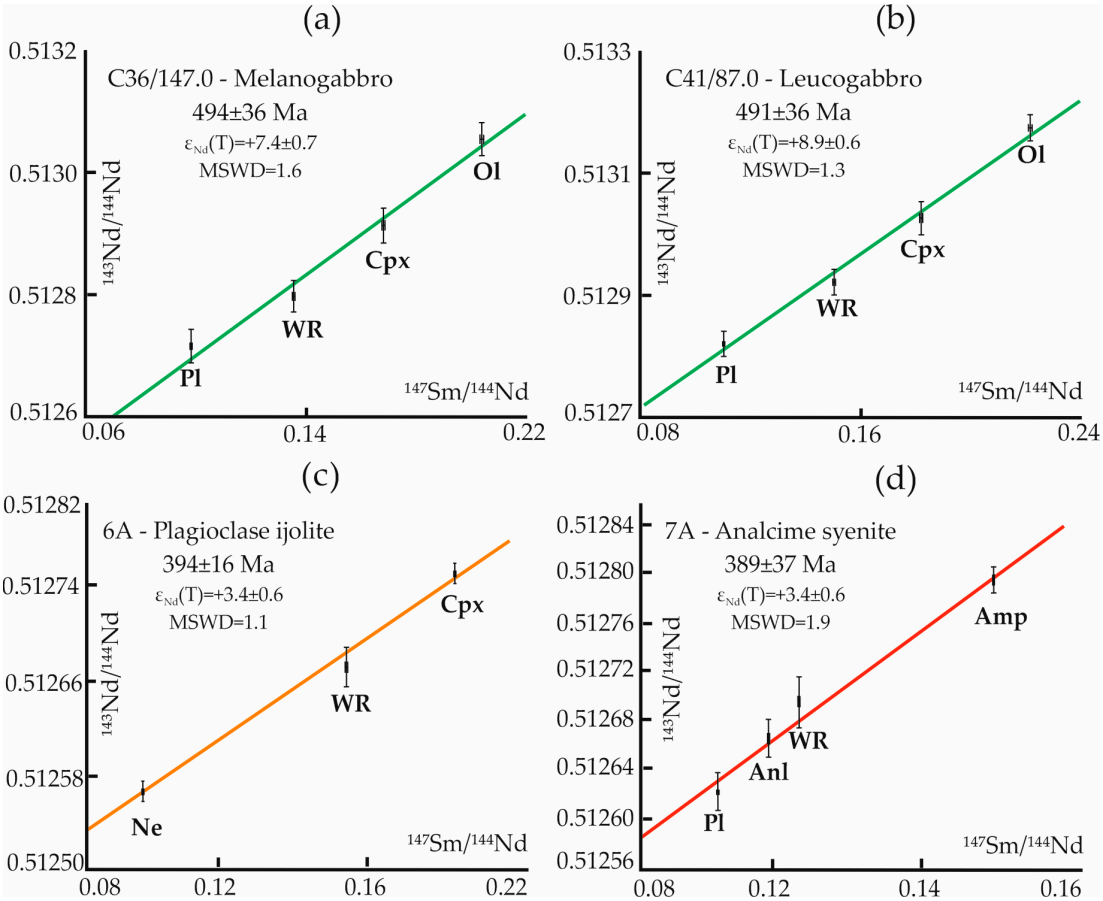

Figure 10. Sm–Nd isochrones for mineral separations and whole rock compositions of the University pluton and crosscutting N-S trending younger swarm of alkaline dikes [72]: (**a**,**b**) subalkaline melanogabbro (sample C36/147.0) and leucogabbro (sample C41/87.0) ca. 490 Ma; (**c**,**d**) plagioclase ijolite (sample 6A) and analcime syenite (globule) in fine-grained ijolite (sample 7A) ca. 390 Ma. Explanations of abbreviations see in Table 1.

5. Discussion

5.1. Magnetic Anomalies of the University Pluton Site and N-S Trending Crosscutting Younger Swarm of Alkaline Dikes

The magnetic data clearly show northwest trending faults bounding the University intrusion. North trending linear positive magnetic anomalies mark dikes cutting the University pluton. In addition to direct geological observations in the form of open mines (ditches and pits) [73], ground magnetic data confirm two intense but narrow (1 km wide) dike belts (swarms) of N-S trends (see note in Figure 4 Foidolite dike).

Drilling of the University pluton (the maximum borehole depth was 160 m) did not yield the expected nepheline ore deposits, but urtite xenoliths were found in trenches to the west of the bodies of subalkaline gabbroids, and in drill-hole number C-46, an urtite-porphyry dike N-trending was found breaking through the Berikul formation (see note in Figure 4 sample C-46 from drill-hole and

Figure 6) [33,56]. We interpreted that the distinct linear anomaly in the western part of the pluton was caused by bodies of urtites, which we discovered for the first time (Boloto intrusion). To what event (ca. 490 Ma or ca. 390 Ma) the Boloto intrusion should be attributed to remained unclear.

5.2. Petrographic Synthesis of the University Pluton

According to geological and petrographic observations, three separate associations can be distinguished among igneous rocks in the University pluton area: (1) subalkaline gabbroids ca. 490 Ma; (2) dikes (N-trending) of basic foidolites, with subordinate amounts of feldspar ca. 390 Ma and (3) dikes (N-trending) of ultrabasic foidolites, characterized by the presence of only nepheline as a salic component ca. 390 Ma. There can be transitional boundaries between these types.

According to geological and petrographic observations in other alkaline-gabbroid plutons of the Kuznetsk Alatau (Figure 1b), in the Belogorskii [8] and Upper Petropavlovka [9] plutons, feldspar ijolites are independent intrusive phases and cut subalkaline gabbroids. At the Kiya-Shaltyrskii deposit [21], urtite bodies are also an independent and later phase. Separated from gabbroids, basic foidolites are represented as separate bodies within the Goryachegorskii pluton (both gradual transitions and intrusive relationships between plagioclase ijolites and feldspar urtites are observed here) [31].

Thus, the alkaline dikes of the N-S trending of the ijolite-porphyry with urtite xenoliths and the dikes of the urtite-porphyry belonging to the University pluton in their petrographic, petrochemical and geochemical composition are identical with the urtites of the Kiya-Shaltyrskii deposit ca. 400 Ma (deposits of rich nepheline ores) [21].

5.3. Magma Sources for the University Pluton and Crosscutting Dikes

The seven alkaline-gabbroid plutons of the northern part of the KA ridge region (Figure 9; as described above) and six of their varieties of igneous rocks (subalkaline gabbroids, ultramafic, basic foidolites, theralites, syenites and carbonatites) were analyzed for Sr and Nd isotopic compositions. The samples show slight variations in radiogenic $\varepsilon_{Nd}(T)$ (from +1.74 to +8.7), but with respect to the radiogenic $\varepsilon_{Sr}(T)$ (from +3.43 to +36.6), the values exhibited a wide range, and a shift was observed in the early intrusive phases of gabbroids to late alkaline dike rocks (Figure 9), from more mantle compositions toward a crustal component and this may indicate active crustal contamination of magma. One of the possible mechanisms of selective crustal contamination during the emplacement of magmas is the thermal mobilization of Sr-rich brines conserved in the Cambrian sedimentary strata of the KA [74,75]. Due to the strong contamination of all igneous rocks by crustal strontium, we assumed that the primary source of the magmatic melt was the plume component of the primitive mantle (PREMA) and these data are consistent with a number of studies [8,9,20,27,74,76]. V.V. Yarmolyuk and V.I. Kovalenko [77] in their work showed that the development of the Early Middle Paleozoic basic magmatism in the northwestern part of the CAOB occurred under the influence of a North-Asian superplume on the lithosphere, which was dominated by PREMA material.

This North-Asian superplume ca. 500 Ma affected the northern part of the KA; Gornaya Shoriya; Batenevskii range; Gorny Altai; Eastern and Southeastern Tuva; Eastern Sayan, Southern Pribaikal'e; Yenisei range; Priolkhon'e; Zabaikal'e, Prikhubsugul'e and Western Mongolia during the period from the Early Cambrian to the Middle Ordovician, producing large volumes of granites and various types of mantle magmatism [20,47,78]. The University pluton, with 494–491 Ma subalkaline gabbroids was part of this superplume event during the accretion of the KA terrane. The next stage was the introduction of an extensive swarm of N-S trending dikes of both alkaline and subalkaline composition 394–389 Ma. Recent studies [43,48] have recognized the large Altai-Sayan rift system (ASRS) and associated Altai-Sayan LIP, which also extend into the KA terrane. The crosscutting N-S striking dikes that cut the University pluton are likely related to the ASRS plume event. For a more detailed determination of the cause-and-effect relationships with certain regional magmatic events, we planned to conduct additional isotopic (Rb-Sr; U-Pb) studies of subalkaline and alkaline intrusions of the University pluton and crosscutting dikes.

5.4. Genetic Nexus of Alkaline-Basic Intrusions in the Kuznetsk Alatau Terrane

For clarity, we presented the age dates of seven complexly differentiated alkaline–basic intrusions of the KA terrane, which were discussed in our studies earlier (Figure 9 and Section 5.3) and this will help to divide the magmatic events of their formation into separate stages of formation (Table 2). Consequently, it will be possible to compare the magmatic events that took place at the University pluton with the events of other alkaline-basic intrusions KA, which will help to reveal the conditions of the formation of the University pluton.

Table 2. Dating of alkaline–basic intrusions in the Kuznetsk Alatau terrane.

Intrusion	Rock Type (Mineral)	Age, Ma	Dating Method	Reference
Upper Petropavlovka	Carbonatite, foidolite; Theralite	509 ± 10 502 ± 46	$^{147}Sm/^{144}Nd$ $^{87}Rb/^{86}Sr$	[9]
University	Subalkaline leucogabbro, Subalkaline melanogabbro	494 ± 36 491 ± 36	$^{147}Sm/^{144}Nd$	[32]
N-S dike swarm crosscutting University pluton	Plagioclase ijolite, Analcime syenite	394 ± 16 389 ± 37	$^{147}Sm/^{144}Nd$	[33]
Kiya-Shaltyrskii	Melanocratic gabbro, Pegmatoid ijolite, Nepheline syenite	406 ± 2 398.9 ± 5.5 387.5 ± 2.8	$^{87}Rb/^{86}Sr$ $^{206}Pb/^{238}U$ $^{206}Pb/^{238}U$	[21]
Belogorskii	Plagioclase ijolite (amphibole), Nepheline syenite (mica)	402.9 ± 3.4 400.6 ± 3.4	$^{40}Ar/^{39}Ar$	[8]
Dedovogorskii	Pegmatoid nepheline syenite (baddeleyite, zircon)	401 ± 2 400.9 ± 6.8	$^{206}Pb/^{238}U$	[21]
Kurgusuyulskii	Juvite	393.6 ± 9.2	$^{206}Pb/^{238}U$	[21]
Goryachegorskii	Foyaite	264.1 ± 1.9	$^{206}Pb/^{238}U$	[31]

Accordingly, as a result of the data from isotope-geochronological studies (Sm-Nd, Rb-Sr, U-Pb and Ar-Ar), alkaline intrusions can be divided into three age groups, corresponding to the Cambrian and Early Ordovician (510–480 Ma), Early and Middle Devonian (410–390 Ma) and Late Permian (265 Ma) [8–12,18,21,27,28,31–33,45,46,48,72].

Events in the Middle-Upper Cambrian, which formed the Upper Petropavlovka alkaline–basic pluton [9] and the subalkaline gabbro University pluton, we associated with the manifestation of the North Asian superplume [23] in the western territory of the CAOB. As a result, this intrusive magmatism of intraplate specificity was widely developed at the initial stage of the accretionary stage of the development of the terrane KA crust, when numerous plutons of alkaline and subalkaline rocks of the region, and picrate and picrodolerite magmatism in the north part Mongolia ca. 500 Ma [23,47,78].

In the KA terrane, the second stage of magmatism consists of Early and Middle Devonian alkaline-basic magmatism forming the Belogorskii [8], Kiya-Shaltyrskii, Dedovogorskii, Kurgusuyulskii plutons [21] and dikes of the N-S trending cutting the University pluton. We associate this event with the emergence of the Altai-Sayan rift system/LIP ca. 400 Ma [43,48].

Additionally, recent U-Pb dating of the foyaite phase of the Goryachegorskii pluton, which cuts only Devonian volcanic sediments, in contrast to other alkaline-basic massifs where they interact with both carbonate and volcanogenic-sedimentary strata, showed its belonging attachment to the late Paleozoic era (Upper Permian Epoch) [21,31]. Apparently, the Goryachegorskii pluton is a product of the bimodal basalt-comendite and basalt-pantellerite volcanic associations, which controlled the distribution of numerous plutons of alkaline granites and syenites in the rift system of Central Asia during the closure of the Paleo-Asian Ocean and collision of the Siberian and North China continents [23].

Conditions for the Formation of the University Pluton in the Kuznetsk Alatau Terrane

Subalkaline gabbro's have LREE patterns (Figure 8) between the oceanic island basalt (OIB) [69] and island arc basalt (IAB) [70] types [69], and HREE with the exception of (Tm ≈ 18.43; Yb ≈ 17.66; Lu ≈ 14.88 ppm), which in turn were more enriched than oceanic islands basalts (Tm ≈ 13.73; Yb ≈ 12.71; Lu ≈ 11.81 ppm). In terms of total REE (∑REE ≈ 226.38 ppm), leucotheralites were more differentiated than subalkaline gabbro the foidolites (of the pluton) and show a similar pattern to OIB, but with a noticeable enrichment in HREE relative to OIB. Foidolites of the pluton were identical in their pattern with subalkaline gabbro, except for a few samples (K55/6; K55/2; U6), which had the lowest REE concentrations (∑REE = 59.91; 95.54; 150.37 ppm; Table S1), less than the IAB [70] standard. The nepheline and alkaline syenites did not differ much from the subalkaline and alkaline units of the pluton, but in two samples (15B; SH-394/4; Figure 6c) the maximum REE concentrations (∑REE = 323; 1566.95 ppm) were found, which exceeded the OIB composition by several hundred times. Comparison of the main varieties of plutonic rocks according to REE revealed a similar distribution, both in the level of accumulation and in the level of fractionation. Among the differences, positive Eu anomalies occurred in the subalkaline leucogabbro (Eu/Eu(n) = +1.25; +1.26 (Figure 3b); +1.45; +1.86), leucotheralites (Eu/Eu(n) = +1.24; Figure 3c) and analcime syenite (Eu/Eu(n) = +1.31; Figure 3g), which is possibly explained by the cumulative segregation of plagioclase as an early crystallizing phase. Negative Eu anomalies were recorded in five samples: foyaite (Eu/Eu(n) = −0.27), pegmatoid nepheline syenite (Eu/Eu(n) = −0.60; Figure 6c), melanogabbro (Eu/Eu(n) = −0.27; −0.65) and leucotheralite (Eu/Eu(n) = −0.78), which is possibly the result of fractional crystallization or partial melting, in which plagioclase remains in the melt source.

The behavior of REE and HFSE in the rocks of the University pluton suggests that the magma sources were heterogeneous. Despite the different degrees of melt differentiation (La/Yb(n) = 0.53–12.72), the geochemical parameters reflected the joint involvement of both OIB and IAB components in melt genesis. Mixing of these components is also noted for a number of other Early and Middle Paleozoic alkaline-basic intrusions of the region, the origin of which is associated with the processes of plume-lithospheric interaction and the inheritance of geochemical signatures of subduction in the products of mantle diapirism [8,9,18,27]. Negative (Nb, Ta, Zr and Hf) anomalies and the enrichment of mobile elements of fluids (Rb, Sr, Ba and U) in the rocks of the studied association indicate a probable interaction of plume melts with lithospheric mantle that was metasomatized during prior subduction events associated with the formation of accretion complexes.

The heterogeneity of the data is confirmed by a number of trace element discrimination diagrams (Th/Yb–Ta/Yb; Th/Ta–La/Yb; Nb/Y–Zr/Y; Tb/Ta(n)–Th/Ta(n); Zr/Nb–Nb/Th and Th/Nb–Ba/La; Figure 11). Subalkaline and alkaline plutonic rocks of the University pluton had within-plate character suggesting a plume source, but occurred in a region with an active continental margin (Figure 11a–d). These processes can be the interaction of plume material with more ancient accretion-collisional complexes on the active margin of the Paleo-Asian Ocean [8,10,20,22,27,31].

Taking into account the increased alumina content and low titanium content of subalkaline and alkaline rocks of the University pluton, and the observed ratios of highly charged elements, with a relative enrichment in rubidium, strontium and uranium, and with a noticeable depletion in niobium and tantalum, these geochemical features collectively indicate a complex geodynamic paleo environment of formation, juxtaposing convergence features of island arc, continental margin and with intraplate magmatism (Figure 11e,f). An example of such a complex combination of tectonic regimes initiating magmatic activity can be the modern active continental margin of the Californian type [79].

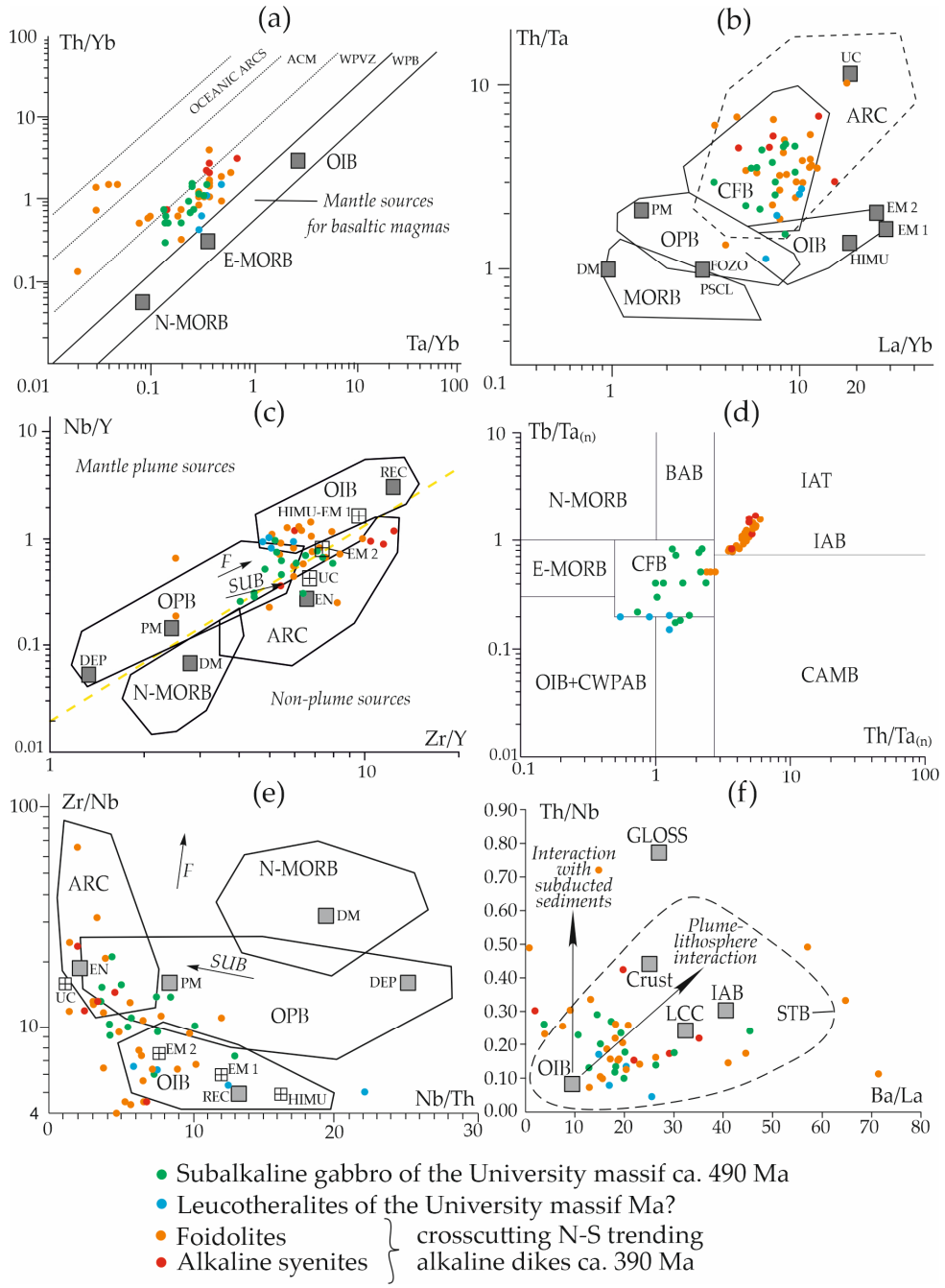

Figure 11. Variation diagrams of HFSE in subalkaline and alkaline rocks of the University pluton. (**a**) Th/Yb–Ta/Yb [80]: Oceanic arcs, ACM = active continental margins, WPVZ = within-plate volcanic zones, WPB = within-plate basalts, OIB = ocean island basalts, E-MORB = "enriched-type" mid-ocean ridge basalts, N-MORB = "normal-type" mid-ocean ridge basalts; (**b**) Th/Ta–La/Yb [81,82]: OPB = oceanic plateau basalt, SZB = subduction zone basalt, UC = upper crust, ARC = subduction zone basalts, CFB = continental flood basalt, PM = primitive mantle, HIMU = type basalt; HIMU = means high μ, where the μ-value is the ratio of $^{238}U/^{204}Pb$. EM I-type basalt and EM II-type basalt = basalts from enriched mantle sources, DM = depleted mantle, FOZO = focal zone; (**c**) Nb/Y–Zr/Y and (**e**) Zr/Nb–Nb/Th [83]: Arrows indicate effects of batch melting (F) and subduction (SUB). DEP = deep depleted mantle, EN = enriched component, REC = recycled component; (**d**) Tb/Ta(n)–Th/Ta(n) [84]: BAB = back-arc basin basalts, IAT = island arc tholeiites, IAB = island arc basalts, CAMB = active continental margin basalts, CWPAB = continental within-plate alkali and transitional basalts, (n) = primitive mantle-normalized [69]; (**f**) Th/Nb–Ba/La [85]: OIB [69], IAB [70], LCC = lower continental crust [86], Crust [87], GLOSS [88], STB = Siberian traps.

The CAOB records convergence and interactions between various types of orogenic components, including arc systems of the Japanese, Mariana and Alaskan-Aleutian types, and active continental margins of the Siberian Craton, which imply wide accretionary complexes and accreted arcs and terranes [25,26,50,89]. In the KA terrane, there can be spatially combined subduction and plume magmatism, recognized by geochemical components from heterogeneous sources [27].

6. Conclusions

Magnetic mapping of the poorly exposed University pluton of the Kuznetsk Alatau ridge, Siberia exhibited positive anomalies of intrusive units of the University pluton against the background of negatively magnetized host rocks (sedimentary rocks of the Ust-Kundat and Berikul formations). The high-intensity positive anomaly in the western part of the study area is probably associated with nepheline mineralization, which may be an analogue of the nearby economically important Kiya-Shaltyrskii nepheline ore deposit in addition, linear (N-trending) positive anomalies are associated with younger crosscutting N-S trending alkaline dikes.

Based on the Sm-Nd age dates presented in this manuscript, the University pluton was likely emplaced at about 490 Ma, which indicates its likely membership in a widespread intraplate event that extends into Mongolia [47]. The University pluton is cut by 390 Ma alkaline N-S trending dikes that likely belong to the regional ca. 400 Ma Altay-Sayan Rift System/LIP [43,48]. As is known, magmatism in the western part of the CAOB had a long history and some events, as in the KA terrane, are associated with the activity of mantle plumes. The broad signature (ε_{Nd}(T) from +1.74 to +8.7 and ε_{Sr}(T) from +3.43 to +36.6) of the isotopic composition of the alkaline-gabbroid association indicates the generation of initial magmas from a plume source of the moderately depleted PREMA mantle, whose derivatives experienced a selective crustal contamination likely through interaction with lithosphere metasomatized during final orogenic assembly of the CAOB.

Supplementary Materials: The following are available online at http://www.mdpi.com/2075-163X/10/12/1128/s1, Table S1: Chemical composition of igneous rocks of the University intrusion.

Author Contributions: A.A.M.: Methodology, research, data supervision, obtaining funding, project administration, idea of writing and preparing an initial project. I.F.G.: Resources, supervision and investigation, fundraising and project administration, review and editing. R.E.E.: Project management, resources, constructive review and editing. P.A.S.: Discussion and interpretation of isotopic geochemistry, verification, review and editing. Y.V.K.: Geophysical survey results discussion, verification, review and editing. All authors have read and agreed to the published version of the manuscript.

Funding: Geochemical study reported was funded by RFBR (project number 19-35-90030). Isotope-geochronological studies by the Sm-Nd method were carried out at the expense of the Russian Science Foundation (project number 18-17-00240) and the Rb-Sr method at the expense of a mega-grant in accordance with the Decree of the Government of the Russian Federation (Agreement number 14.Y26.31.0012). Clarification of the geological structure of the University pluton was carried out at the expense of the State Task of the Ministry of Science and Higher Education of the Russian Federation (project number 0721-2020-0041).

Acknowledgments: The authors are grateful to the staff of the National Research Tomsk State University (Tomsk, Russia) for many years of participation in expeditions, analytical studies and consultations on magmatic petrology and isotopic geochemistry, as well as to colleagues from the Geological Institute—subdivision of the Federal Research Centre, Kola Science Centre of the Russian Academy of Sciences (Apatity, Russia) and the Institute of Geology and Mineralogy V.S. Sobolev of the Siberian Branch of the Russian Academy of Sciences (Novosibirsk, Russia).

Conflicts of Interest: The authors declare that there is no conflict of interest.

References

1. Sheimann, Y.M.; Apeltsin, F.R.; Nechaeva, E.A. *Alkaline Intrusions, Their Placement and Associated Mineralization*; Gosgeoltekhizdat: Moscow, Russia, 1961; pp. 1–176. (In Russian)
2. Sheimann, Y.M. *Essays on Deep Geology*; Nedra: Moscow, Russia, 1968; pp. 1–232. (In Russian)
3. Yashina, R.M. *Alkaline Magmatism in Orogenic Areas (Case of the Southern Periphery of the Siberian Craton)*; Nauka: Moscow, Russia, 1982; pp. 1–274. (In Russian)

4. Burke, K.; Dewey, J. Plume-generated triple junctions: Key indicators in applying plate tectonics to old rocks. *J. Geol.* **1973**, *81*, 406–433. [CrossRef]
5. Pirajno, F. Intracontinental anorogenic alkaline magmatism and carbonatites, associated mineral systems and the mantle plume connection. *Gondwana Res.* **2015**, *1328*, 1–36. [CrossRef]
6. Condie, K.C. *Mantle Plumes and Their Record in Earth History*; Cambridge University Press: Cambridge, UK, 2001; pp. 1–305.
7. Ernst, R.E. *Large Igneous Provinces*; Cambridge University Press: Cambridge, UK, 2014; pp. 1–667.
8. Vrublevskii, V.V.; Grinev, O.M.; Izokh, A.E.; Travin, A.V. Geochemistry, isotope triad (Nd–Sr–O), and ^{40}Ar–^{39}Ar age of Paleozoic alkaline mafic intrusions of the Kuznetsk Alatau (by the example of the Belaya Gora pluton). *Russ. Geol. Geophys.* **2016**, *57*, 592–602. [CrossRef]
9. Vrublevskii, V.V. Sources and geodynamic setting of petrogenesis of the Middle Cambrian Upper Petropavlovka alkaline basic pluton (Kuznetsk Alatau, Siberia). *Russ. Geol. Geophys.* **2015**, *56*, 379–401. [CrossRef]
10. Vrublevskii, V.V.; Gertner, I.F.; Tishin, P.A.; Bayanova, T.B. Age range of zircon and sources of alkaline rocks Kurgusul intrusive, Kuznetsk Alatau: First U–Pb (Shrimp 2) Isotope and Sm–Nd Data. *Dokl. Earth Sci.* **2014**, *459*, 601–606. (In Russian) [CrossRef]
11. Vrublevskii, V.V.; Krupchatnikov, V.I.; Izokh, A.E.; Gertner, I.F. Alkaline Rocks and Carbonatites of Gorny Altai (Edelweiss complex): Indicator of Early Paleozoic Pluma Magmatism in the Central Asian Folding Belt. *Russ. Geol. Geophys.* **2012**, *53*, 945–963.
12. Vrublevskii, V.V.; Izokh, A.E.; Polyakov, G.V.; Gertner, I.F.; Yudin, D.S.; Krupchatnikov, V.I. Early Paleozoic alkaline magmatism of Gorny Altai: ^{40}Ar-^{39}Ar-Geochronological evidence of the Edelweiss complex. *Dokl. Earth Sci.* **2009**, *427*, 96–100. [CrossRef]
13. Doroshkevich, A.G.; Ripp, G.S.; Izbrodin, I.A.; Savatenkov, V.M. Alkaline magmatism of the Vitim province, West Transbaikalia, Russia: Age, mineralogical, geochemical and isotope (O, C, D, Sr and Nd) data. *Lithos* **2012**, *152*, 157–172. [CrossRef]
14. Doroshkevich, A.G.; Izbrodin, I.A.; Rampilov, M.O.; Ripp, G.S.; Lastochkin, E.I.; Khubanov, V.B. Permo–Triassic stage of alkaline magmatism in the Vitim plateau (western Transbaikalia). *Russ. Geol. Geophys.* **2018**, *59*, 1061–1077. [CrossRef]
15. Vrublevskii, V.V.; Morova, A.A.; Bukharova, O.V.; Konovalenko, S.I. Mineralogy and Geochemistry of Triassic Carbonatites in the Matcha Alkaline Intrusive Complex (Turkestan-Alai Ridge, Kyrgyz Southern Tien Shan), SW Central Asian Orogenic Belt. *J. Asian Earth Sci.* **2017**, *153*, 252–281. [CrossRef]
16. Gordienko, I.V. Relationship between subduction related and plume magmatism at the active boundaries of lithospheric plates in the interaction zone of the Siberian continent and Paleoasian Ocean in the Neoproterozoic and Paleozoic. *Geodyn. Tectonophys.* **2019**, *10*, 405–457. (In Russian) [CrossRef]
17. Gordienko, I.V.; Metelkin, D.V. The evolution of the subduction zone magmatism on the Neoproterozoic and Early Paleozoic active margins of the Paleoasian. *Ocean. Russ. Geol. Geophys.* **2016**, *57*, 69–81. [CrossRef]
18. Makarenko, N.A.; Kotel'nikov, A.D. The Kashpar Cambrian-Ordovik gabbro-diorite-quartzmontsodiorite-syenite Complex-New Petrography Department on the Eastern Slope of the Kuznetsk Alatau. *Geosph. Stud.* **2018**, *2*, 52–71. (In Russian)
19. Doroshkevich, A.G.; Ripp, G.S.; Sergeev, S.A.; Konopel'ko, D.L. The U-Pb geochronology of the Mukhal alkaline massif (*Western Transbaikalia*). *Russ. Geol. Geophys.* **2012**, *53*, 69–81. [CrossRef]
20. Vrublevskii, V.V.; Gertner, I.F.; Ernst, R.E.; Izokh, A.E.; Vishnevskii, A.V. The Overmaraat-Gol Alkaline Pluton in Northern Mongolia: U–Pb Age and Preliminary Implications for Magma Sources and Tectonic Setting. *Minerals* **2019**, *9*, 170. [CrossRef]
21. Vrublevskii, V.V.; Gertner, I.F.; Gutiérrez-Alonso, G.; Hofmann, M.; Grinev, O.M.; Tishin, P.A. Isotope (U-Pb, Sm–Nd, Rb–Sr) geochronology of alkaline basic plutons of the Kuznetsk Alatau. *Russ. Geol. Geophys.* **2014**, *55*, 1264–1277. [CrossRef]
22. Kuzmin, M.A.; Yarmolyuk, V.V. Mantle plumes of Central Asia (Northeast Asia) and their role in forming endogenous deposits. *Russ. Geol. Geophys.* **2014**, *55*, 120–143. [CrossRef]
23. Yarmolyuk, V.V.; Kuzmin, M.I.; Vorontsov, A.A. West Pacific-type convergent boundaries and their role in the formation of the Central Asian Fold Belt. *Russ. Geol. Geophys.* **2013**, *54*, 1427–1441. [CrossRef]

24. Izbrodin, I.; Doroshkevich, A.; Rampilov, M.; Elbaev, A.; Ripp, G. Late Paleozoic alkaline magmatism in Western Transbaikalia, Russia: Implications for magma sources and tectonic settings. *Geosci. Front.* **2020**, *11*, 1289–1303. [CrossRef]
25. Pirajno, F.; Santosh, M. Rifting, intraplate magmatism, mineral systems and mantle dynamics in central-east Eurasia: An overview. *Ore Geol. Rev.* **2014**, *63*, 265–295. [CrossRef]
26. Wilhem, C.; Windley, B.F.; Stampfli, G.M. The Altaids of Central Asia: A tectonic and evolutionary innovative review. *Earth Sci. Rev.* **2012**, *113*, 303–341. [CrossRef]
27. Vrublevskii, V.V.; Kotel'nikov, A.D.; Izokh, A.E. The age and petrologic and geochemical conditions of formation of the Kogtakh gabbro-monzonite complex in the Kuznetsk Alatau. *Russ. Geol. Geophys.* **2018**, *59*, 718–744. [CrossRef]
28. Vrublevskii, V.V.; Kotel'nikov, A.D.; Rudnev, S.N.; Krupchatnikov, V.I. Evolution of the Paleozoic granitoid magmatism in the Kuznetsk Alatau: New geochemical and U-Pb (SHRIMP-II) isotope data. *Russ. Geol. Geophys.* **2016**, *57*, 225–246. [CrossRef]
29. Metelkin, D.V.; Koz'min, D.G. Paleomagnetic characteristic of Cambria Batenevskii range: On the question of the evolution of the Kuznetsk-Alatau island arc in the south of Siberia. *Russ. Geol. Geophys.* **2012**, *53*, 50–66. (In Russian) [CrossRef]
30. Doroshkevich, A.G.; Veksler, I.V.; Klemd, R.; Khromova, E.A.; Izbrodin, I.A. Trace-element composition of minerals and rocks in the Belaya Zima carbonatite complex (Russia): Implications for the mechanisms of magma evolution and carbonatite formation. *Lithos* **2017**, *284*, 91–108. [CrossRef]
31. Vrublevskii, V.V.; Gertner, I.F.; Gutiérrez-Alonso, G.; Hofmann, M.; Grinev, O.M.; Mustafaev, A. Multiple intrusion stages and mantle sources of the Paleozoic Kuznetsk Alatau alkaline province, Southern Siberia: Geochemistry and Permian U–Pb, Sm–Nd ages in the Goryachegorsk ijolite-foyaite intrusion. *Int. Geol. Rev.* **2020**. [CrossRef]
32. Mustafayev, A.A.; Gertner, I.F.; Serov, P.A. Features of geology and composition of rocks from the alkaline-gabbroic University massif (NE Kuznetsk Alatau ridge, Siberia). *Earth Envir. Sci.* **2017**, *319*, 1–13.
33. Mustafaev, A.; Gertner, I. Isotope-geochemical (Sm–Nd, Rb–Sr, REE, HFSE) composition of the University foidolite-gabbro pluton, Kuznetsk Alatau ridge, Siberia. *Vestn. St. Petersburg Univer. Earth Sci.* **2020**, *65*, 1–33. (In Russian) [CrossRef]
34. Sengör, A.C.; Natal'in, B.A.; Burtman, V.S. Evolution of the Altaid tectonic collage and Palaeozoic crustal growth in Eurasia. *Nature* **1993**, *364*, 299–306. [CrossRef]
35. Windley, B.F.; Alexeiev, D.V.; Xiao, W.; Kröner, A.; Badarch, G. Tectonic models for accretion of the Central Asian Orogenic Belt. *J. Geol. Soc. Lond.* **2007**, *164*, 31–47. [CrossRef]
36. Coleman, R.G. Continental growth of North West China. *Tectonics* **1989**, *8*, 621–635. [CrossRef]
37. Dobretsov, N.L.; Buslov, M.M.; Vernikovsky, V.V. Neoproterozoic to Early Ordovician Evolution of the Paleo-Asian Ocean: Implications to the Break-up of Rodinia. *Gondwana Res.* **2003**, *6*, 143–159. [CrossRef]
38. Kovalenko, V.I.; Yarmolyuk, V.V.; Kovach, V.P.; Kotov, A.B.; Kozakov, I.K.; Salnikova, E.B.; Larin, A.M. Isotope provinces, mechanisms of generation and sources of the continental crust in the Central Asian mobile belt: Geological and isotopic evidence. *Asian Earth Sci.* **2004**, *23*, 605–627. [CrossRef]
39. Kröner, A.; Hegner, E.; Lehmann, B.; Heinhorst, J.; Wingate, M.T.D.; Liu, D.Y.; Ermelov, P. Palaeozoic arc magmatism in the Central Asian Orogenic Belt of Kazakhstan: SHRIMP zircon ages and whole-rock Nd isotopic systematics. *Asian Earth Sci.* **2008**, *32*, 118–130. [CrossRef]
40. Rytsk, E.Y.; Kovach, V.P.; Yarmolyuk, V.V.; Kovalenko, V.I. Structure and evolution of the continental crust in the Baikal Fold Region. *Geotectonic* **2007**, *41*, 440–464. [CrossRef]
41. Windley, B.F.; Kröner, A.; Guo, J.; Qu, G.; Li, Y.; Zhang, C. Neoproterozoic to Paleozoic geology of the Altai orogen, NW China: New zircon age data and tectonic evolution. *J. Geol.* **2002**, *110*, 719–739. [CrossRef]
42. Kröner, A.; Kovach, V.; Belousova, E.; Hegner, E.; Armstrong, R.; Dolgopolova, A.; Sun, M. Reassessment of continental growth during the accretionary history of the Central Asian Orogenic Belt. *Gondwana Res.* **2014**, *25*, 103–125. [CrossRef]
43. Vorontsov, A.; Yarmolyuk, V.; Dril, S.; Ernst, R.; Perfilova, O.; Grinev, O.; Komaritsyna, T. Magmatism of the Devonian Altai-Sayan Rift System: Geological and geochemical evidence for diverse plume-lithosphere interactions. *Gondwana Res.* **2020**, *89*, 193–219. [CrossRef]

44. Shokal'skii, S.P.; Babin, G.A.; Vladimirov, A.G.; Borisov, S.M.; Gusev, N.I.; Tokarev, V.N.; Kruk, N.N. *Correlation of Igneous and Metamorphic Complexes in the Western Altai–Sayan Folded Area*; SO RAN: Novosibirsk, Russia, 2000; pp. 1–188. (In Russian)
45. Kononova, V.A. *Jakupirangite-Urtite Series of Alkaline Rocks*; Nauka: Moscow, Russia, 1976; pp. 1–215. (In Russian)
46. Andreeva, E.D.; Kononova, V.A.; Sveshnikova, E.V.; Yashina, R.M. Alkaline rocks. In *Igneous Rocks*; Bogatikov, O.A., Kononova, V.A., Borsuk, A.M., Gon'shakova, V.I., Kovalenko, V.I., Laz'ko, E.E., Sharkov, E.V., Eds.; Nauka: Moscow, Russia, 1984; Volume 2, pp. 1–415. (In Russian)
47. Izokh, A.E.; Vishnevskii, A.V.; Polyakov, G.V.; Shelepaev, R.A. Age of picrite and picrodolerite magmatism in western Mongolia. *Russ. Geol. Geophys.* **2011**, *52*, 7–23. [CrossRef]
48. Ernst, R.E.; Rodygin, S.A.; Grinev, O.M. Age correlation of Large Igneous Provinces with Devonian biotic crises. *Glob. Planet. Chang.* **2020**, *185*, 103097. [CrossRef]
49. Jahn, B.-M.; Wu, F.Y.; Chen, B. Massive granitoid generation in Central Asia: Nd isotope evidence and implication for continental growth in the Phanerozoic. *Episodes* **2000**, *23*, 82–92. [CrossRef]
50. Xiao, W.; Santosh, M. The western Central Asian Orogenic Belt: A window to accretionary orogenesis and continental growth. *Gondwana Res.* **2014**, *25*, 1429–1444. [CrossRef]
51. Babin, G.A.; Yuriev, A.A.; Bychkov, A.I. *State Geological Map of the Russian Federation. Scale 1:1,000,000 (Third Generation). Sheet N-45 (Novokuznetsk)*; VSEGEI: Saint Petersburg, Russia, 2007. (In Russian)
52. Kortusov, M.P. *Paleozoic Intrusive Complexes of the Mariinsky Taiga (Kuznetsk Alatau). Tom 1*; Izd. Tomsk Univers: Tomsk, Russia, 1967; pp. 1–163. (In Russian)
53. Alabin, L.V. *Structural-Formational and Metallogenic Zoning of the Kuznetsk Alatau*; Nauka: Novosibirsk, Russia, 1983; pp. 1–102. (In Russian)
54. Esin, S.V.; Korchagin, S.A.; Esina, O.A.; Gertner, I.F. *Alkaline and subalkaline rocks of the Kuznetsk Alatau. Nepheline Ore-Bearing Rocks of Universitetskii 1 and 2 Sites (Kuznetsk Alatau)*; Izd. Tomsk Univers: Tomsk, Russia, 1987; pp. 74–82. (In Russian)
55. Osipov, P.V.; Makarenko, N.A.; Korchagin, S.A.; Gertner, I.F.; Grinev, O.M. New alkaline-gabbroid ore-bearing massif in the Kuznetsk Alatau. *Russ. Geol. Geophys.* **1989**, *11*, 79–82. (In Russian)
56. Korchagin, S.A.; Gertner, I.F. *Report on the Search for Naturally Rich and Easily Ore-Rich Nepheline Ores within the Universitetskii 1 and 2, Voskresenka and Bezymyanka Sites Conducted by the Martaiga Expedition in 1983–1987*; Martaiga: Novokuznetsk, Russia, 1987. (In Russian)
57. Karmanova, N.G.; Karmanov, N.S. Universal XRF silicate analysis of rocks using the ARL-9900XP spectrometer. In *All-Russian Conference on X-ray Spectral Analysis No. 7*; IGM SB RAS: Novosibirsk, Russia, 2011; 126p. (In Russian)
58. Anoshkina, Y.V.; Asochakova, E.M.; Bukharova, O.V.; Tishin, P.A. Improvement of schemes for chemical sample preparation of carbonaceous rocks with subsequent analysis of high-charge elements by inductively coupled plasma mass spectrometry. *Bull. TSU* **2012**, *359*, 178–181. (In Russian)
59. Serov, P.A.; Ekimova, N.A.; Bayanova, T.B.; Mitrofanov, F.P. Sulfide minerals—New geochronometers during Sm-Nd dating of ore genesis of stratified mafic-ultramafic intrusions of the Baltic Shield. *Lithosphere* **2014**, *4*, 11–21. (In Russian)
60. Tanaka, T.; Togashi, S.; Kamioka, H.; Amakawa, H.; Kagami, H.; Hamamoto, T.; Kunimaru, T. JNdi-1: A neodymium isotopic reference in consistency with LaJolla neodymium. *Chem. Geol.* **2000**, *168*, 279–281. [CrossRef]
61. Raczek, I.; Jochum, K.P.; Hofmann, A.W. Neodymium and strontium isotope data for USGS reference materials BCR-1, BCR-2, BHVO-1, BHVO-2, AGV-1, AGV-2, GSP-1, GSP-2 and eight MPI-DING reference glasses. *Geostand. Geoanal. Res.* **2003**, *27*, 173–179. [CrossRef]
62. Steiger, R.H.; Jäger, E. Subcommission on geochronology: Convention on the use of decay constants in geo- and cosmochronology. *Earth Planet. Sci. Lett.* **1977**, *36*, 359–362. [CrossRef]
63. Bouvier, A.; Vervoort, J.D.; Patchett, P.J. The Lu–Hf and Sm–Nd isotopic composition of CHUR: Constraints from unequilibrated chondrites and implications for the bulk composition of terrestrial planets. *Earth Planet. Sci. Lett.* **2008**, *273*, 48–57. [CrossRef]
64. Faure, G. *Principles of Isotope Geology*; John Wiley & Sons: New York, NY, USA, 1986; pp. 132–155.
65. York, D. Least squares fitting of straight line. *Canad. J. Phys.* **1966**, *44*, 1079–1086. [CrossRef]

66. Ludwig, K.R. User's Manual for Isoplot/Ex, Version 2.10. In *A Geochronological Toolkit for Microsoft Excel*; Berkley Geochronology Center Special Publication: Berkeley, CA, USA, 1999; Volume 1, pp. 1–46.
67. Middlemost, E.A.K. Naming materials in the magma/igneous rock system. *Earth-Sci. Rev.* **1994**, *37*, 215–244. [CrossRef]
68. Le Maitre, M.J.; Streckeisen, A.; Zanettin, B.; Le Bas, M.J.; Bonin, B.; Bateman, P.; Lameyre, J. *Igneous Rocks*; Cambridge University Press: Cambridge, UK, 2002; pp. 21–29.
69. Sun, S.; McDonough, W.F. Chemical and Isotopic Systematics of Oceanic Basalts: Implications for mantle Composition and Processes. In *Magmatism in the Ocean Basins*; Saunders, A.D., Norry, M.J., Eds.; Geological Society: London, UK, 1989; Volume 42, pp. 313–345.
70. Kelemen, P.B.; Hanghøj, K.; Greene, A.R. One View of the Geochemistry of Subduction-Related Magmatic Arcs, with an Emphasis on Primitive Andesite and Lower Crust. In *Treatise on Geochemistry*; Holland, Y.D., Turekian, K.K., Eds.; Elsevier Ltd.: Amsterdam, The Netherlands, 2003; Volume 3, pp. 593–659.
71. Zindler, A.; Hart, S.R. Chemical geodynamics. *Annu. Rev. Earth Planet. Sci.* **1986**, *14*, 493–571. [CrossRef]
72. Mustafayev, A.A.; Gertner, I.F.; Serov, P.A. New Sm-Nd isotopic data on the University alkaline-gabbro massif (NE Kuznetsk Alatau). In *LIP through Earth History: Mantle Plumes, Supercontinents, Climate Change, Metallogeny and Oil-Gas, Planetary Analogues*; Tomsk CNTI: Tomsk, Russia, 2019; pp. 90–92.
73. Makarenko, N.A.; Osipov, P.V.; Grinev, O.M.; Nomokonova, G.G.; Rihvanov, L.P. *Geological and Geophysical Features of the Ore-Bearing Alkaline-Gabbro Massifs of the Mariinsky Taiga and the Criteria for the Control. of Nepheline Mineralization*; VINITI: Lubercy, Russia, 1988; pp. 1–180. (In Russian)
74. Pokrovsky, B.G. *Crustal Contamination of Mantle Magmas According to Isotope Geochemistry*; Nauka: Moscow, Russia, 2000; pp. 1–223. (In Russian)
75. Vrublevskii, V.V.; Gertner, I.F.; Vladimirov, A.G.; Rudnev, S.N.; Borisov, S.M.; Levchenkov, O.A.; Voitenko, D.N. Geochronological boundaries and geodynamic interpretation of the alkaline mafic magmatism in Kuznetsk Alatau. *Dokl. Earth Sci.* **2004**, *398*, 990–994. (In Russian)
76. Pokrovskii, B.G.; Andreeva, E.D.; Vrublevskii, V.V.; Grinev, O.M. Contamination mechanisms of alkaline-gabbro intrusions in the southern periphery of the Siberian craton: Evidence from strontium and oxygen isotopic compositions. *Petrologiya* **1998**, *6*, 237–251. (In Russian)
77. Yarmolyuk, V.V.; Kovalenko, V.I.; Kovach, V.P.; Kozakov, I.K.; Kotov, A.B.; Sal'nikova, E.B. Geodynamics of caledonides in the Central Asian foldbelt. *Dokl. Earth Sci.* **2003**, *389A*, 311–316. (In Russian)
78. Izokh, A.E.; Polyakov, G.V.; Shelepaev, R.A.; Vrublevskii, V.V.; Egorova, V.V.; Rudnev, S.N.; Lavrenchuk, A.V.; Borodina, E.V.; Oyunchimeg, T. Early Paleozoic Large Igneous Province of the Central Asia Mobile Belt. 2008. Available online: http://www.largeigneousprovinces.org/08may (accessed on 13 December 2020).
79. Cole, R.B.; Stewart, B.W. Continental margin volcanism at sites of spreading ridge subduction: Examples from southern Alaska and western California. *Tectonophysics* **2009**, *464*, 118–136. [CrossRef]
80. Gorton, M.P.; Schandl, E.S. From continents to island arcs: A geochemical index of tectonic setting for arc-related and within-plate felsic to intermediate volcanic rocks. *Can. Miner.* **2000**, *38*, 1065–1073. [CrossRef]
81. Tomlinson, K.Y.; Condie, K.C. Archean mantle plumes: Evidence from greenstone belt geochemistry. *Spec. Pap. Geol. Soc. Am.* **2001**, *352*, 341–358.
82. Ernst, R.E.; Buchan, K.L. Recognizing Mantle Plumes in the Geological Record. *Ann. Rev. Earth Planet. Sci.* **2003**, *31*, 469–523. [CrossRef]
83. Condie, K.C. High field strength element ratios in Archean basalts: A window to evolving sources of mantle plumes? *Lithos* **2005**, *79*, 491–504. [CrossRef]
84. Thièblemont, D.; Chèvremont, P.; Castaing, C.; Triboulet, C.; Feybesse, J.L. The geotectonic discrimination of basic magmatic rocks from trace elements. Re-appraisal from a data base and application to the Pan-African belt of Togo. *Geodyn. Acta* **1994**, *7*, 139–157. [CrossRef]
85. Kuzmichev, A.B.; Pease, V.L. Siberian trap magmatism on the New Siberian Islands: Constraints for Arctic Mesozoic plate tectonic reconstructions. *J. Geol. Soc.* **2007**, *164*, 959–968. [CrossRef]
86. Rudnick, R.L.; Gao, S. *Composition of the Continental Crust*; Holland, Y.D., Turekian, K.K., Eds.; Treatise on Geochemistry; Elsevier Ltd.: Amsterdam, The Netherlands, 2003; Volume 3, pp. 1–64.
87. Weaver, B.L. The origin of ocean island basalt end-member compositions: Trace element and isotopic constraints. *Earth Planet. Sci. Lett.* **1991**, *104*, 381–397. [CrossRef]
88. Stracke, A.; Bizimis, M.; Salters, V.J.M. Recycling oceanic crust: Quantitative constraints. *Geochem. Geophys. Geosyst.* **2003**, *4*, 1–33. [CrossRef]

89. Xiao, W.J.; Windley, B.F.; Allen, M.; Han, C.M. Paleozoic multiple accretionary and collisional tectonics of the Chinese Tianshan orogenic collage. *Gondwana Res.* **2013**, *23*, 1316–1341. [CrossRef]